FOLIA HISTOCHEMICA ET CYTOBIOLOGICA
Vol. 48, No. 3, 2010
pp. 377-386

Doxorubicin-induced F-actin reorganization in cofilin-1 (nonmuscle) down-regulated CHO AA8 cells

Grzanka D.[1], Marszałek A.[1,4], Gagat M.[2], Izdebska M.[2], Gackowska L.[3], Grzanka A.[2,5]

[1]Department of Clinical Pathomorphology, Nicolaus Copernicus University in Toruń, Collegium Medicum in Bydgoszcz, Bydgoszcz, Poland
[2]Department of Histology and Embryology, Nicolaus Copernicus University in Toruń, Collegium Medicum in Bydgoszcz, Bydgoszcz, Poland
[3]Department of Immunology, Nicolaus Copernicus University in Toruń, Collegium Medicum in Bydgoszcz, Bydgoszcz, Poland
[4]Department of Clinical Pathomorphology, Poznan University of Medical Sciences, Poznan, Poland
[5]University of Bydgoszcz, Bydgoszcz, Poland

Abstract: The actin cytoskeleton plays an important role in many cellular processes, including cell mortality, mitosis, cytokinesis, intracellular transport, endocytosis and secretion but also is involved in gene transcription. The dynamics of the actin cytoskeleton is controlled by different classes of actin-binding proteins (ABPs) which regulate the polymerization of actin filaments. In this report we used siRNA against cofilin-1 (nonmuscle) to demonstrate the effect of cofilin on the nuclear and cytoplasmic actin pools in CHO AA8 cells after exposition to various concentrations of doxorubicin. The immunofluorescence studies showed doxorubicin dose dependent tendency to formation the multinucleated giant cells, but also the increase of fluorescence intensity of cofilin in nuclei of untransfected cells. Induction of cell death with doxorubicin treatment in untransfected cells revealed both mitotic catastrophe (in both lower and higher doxorubicin doses) and apoptosis (mostly in higher doxorubicin doses), whereas among cofilin-1 down-regulated cells we observed only mitotic catastrophe. The results suggest that cofilin has apoptosis-inducing ability and that mitotic catastrophe is independent from F-actin content in cell nucleus. In this point of view we conclude that different mechanisms of chromatin reorganization are involved in these two processes. Moreover, we suppose that apoptosis and mitotic catastrophe are independent from each other.

Key words: actin, cof ilin, siRNA, mitotic catastrophe, apoptosis, CHO AA8

Introduction

Actin as the major component of the cytoskeleton in eukaryotic cells is involved in cell locomotion, changes in cell shape, membrane ruffling and formation of lamellipodia [1-3]. We believe, that the dynamic structure and function of actin filaments can be drug targeting agents in cells. Moreover, actin plays a crucial role in many processes *e.g.* cell death, cancer transformation and cell motility [4-8]. The link between actin and cell death might offer opportunities for therapeutic intervention in the future, such as the treatment of cancer and other disorders. Understanding the molecular control of cell death but also signaling to the actin cytoskeleton, involved in apoptosis and other kinds of cell death, will undoubtedly yield a new generation of drug targets in the future. We think that the actin system may be regarded as an additional pathway involved in the process of cell death and can be promising target for development of new chemotherapies. Our previous observations in different cell lines treated with various cytostatic drugs, including doxorubicin [9-11], prompted us to analyze the expression of cofilin and its correlation with actin cytoskeleton reorganization in doxorubicin-induced modes of cell death (apoptosis and mitotic catastrophe) in CHOAA8 cell line.

Correspondence: D. Grzanka, Dept. of Clinical Pathomorphology, Nicolaus Copernicus University in Toruń, Collegium Medicum in Bydgoszcz, Sklodowskiej-Curie Str. 9, 85-094 Bydgoszcz, Poland; e-mail: d_gr@wp.pl

Folia Histochem Cytobiol. 2010:48(3): 377 (377-386)
10.2478/v10042-010-0072-5

The presence of actin in the cell nucleus is also one of the main areas of our studies. In our previous reports, we showed F-actin in the nuclei of various cell lines treated with different cytostatics including doxorubicine [9-11]. For a long time the nuclear existence of actin has been questioned. It also has been suggested that nuclear actin is predominately composed of G-actin [12]. However, some papers showed occurrence of F-actin in the nuclei [13-15].

The cytoplasmic actin is well documented, but there are data showing that actin is translocated into nucleus by cofilin [16-19]. Abe *et al*. showed that cofilin contains a classical bipartite SV40-type nuclear localization sequence (NSL) [18].

However, it is still unclear whether cofilin mediate active transport of actin to nucleus under physiological conditions [20]. Cofilin, a ubiquitous actin-binding protein (ABP) plays a role in regulation of the actin dynamics by promoting the depolymerization of actin filaments [21-22]. In spite of that, further studies are essential to understand the biological function of cofilin in nuclear actin regulation, particularly in the circumstances of active death of cell. There are studies showing that cells with unrepaired DNA damages are eliminated by different types of cell death [23-27]. Our data showed that cells can be destroyed not only by apoptosis but also by other mode of cell death - the mitotic cell death (MCD). In our previous studies we have found that CHO AA8 cells treated with doxorubicin died mostly by cell response known as mitotic catastrophe [28-30]. There are some reports on evaluation of mitotic catastrophe [26,31-33]. Presently, mitotic catastrophe is described as a closing stage of abnormal mitosis with giant multimicronucleated cells [26-27,34-38].

Continuing our studies, here we wanted to provide further evidence for the relation between expression of cofilin and organization of actin in the context of its potential involvement in death processes, apoptosis and mitotic catastrophe, induced in CHOAA8 cell line with different doses of doxorubicin. To elucidate the role of cofilin in F-actin dynamics we used siRNA method to knock-down cofilin expression.

Materials and methods

Cell culture and treatment. The Chinese hamster ovary cell line, kindly provided by Prof. M. Z. Zdzienicka (Department of Molecular Cell Genetics, Nicolaus Copernicus University in Toruń, Collegium Medicum in Bydgoszcz, Poland), was cultured in minimum essential medium eagle (MEM; Sigma Aldrich) supplemented with 10% fetal bovine serum (Gibco) and 50 μg/ml gentamycin in 5% CO_2 at 37°C. For induction of cell death, CHO AA8 cells were treated with different doxorubicin concentrations: 0.5 μM, 1 μM and 2.5 μM for 24 h. After this time period, the medium containing indicated doxorubicin concentrations was replaced with drug-free medium. The cells were cultured for another 48h period in fresh medium. In the $siRNA_{Cfl1}$ treated cells, doxorubicin were added 24 h after transfection. Control cells were grown in the same conditions without doxorubicin addition.

siRNA transfection. 1×10^5 cells were plated onto a 6-well plate in 2 ml of medium without antibiotics and allowed to attach for 24 h. siRNA (corresponding to sequence: 5'-CAG AAG AAG TGA AGA AAC GCA-3') obtained by Qiagen were transfected using the X-tremeGENE siRNA Transfection Reagent (Roche) according to the manufacturer's instructions. To determine the efficiency of $siRNA_{Cfl1}$ transfection, CHO AA8 cells were transfected with varied ratios transfection reagent (μl) to siRNA (μg) (20:4.5:1, and 2:0.4) for 0, 24, 48, and 72 h, respectively. After treatment for the indicated time period, cells were collected for further investigation. The authors found that 72 h transfection with 20:4 ratio of tansfection reagent to siRNA was sufficient to inhibit cofilin expression. Briefly, 20 μl X-tremeGENE siRNA Transfection Reagent was diluted in 80 μl serum free (SF) medium without antibiotics and subsequently, a mixture of 13.48 μl of siRNA and 100 μl of SF medium without antibiotics was added and incubated for 20 min. The mixture was added dropwise to each well containing 1100 μl medium without antibiotics, mixed gently, and then 700 μl medium without antibiotics was added. The final concentration of siRNA in each well of 6-well plate was 130 nM. To minimize the cytotoxicity and avoid an infection, the medium was changed to 5000 μl of fresh culture medium containing antibiotics 24 h after transfection. For determining unspecific effects of siRNA tranfection the nontargeting AllStars negative control siRNA (Qiagen) was used.

Western blot analysis. Whole cell extracts were prepared from cultured cells by homogenizing cells in a lysis buffer containing 50mM Tris-HCl (pH 7.6), 0.1% Triton X-100, 5mM 2-mercaptoethanol, 5 mM EDTA, on ice. After centrifugation of the homogenate (300 × g for 10 min.), supernatants were recovered and used for immunoblot analysis. Bradford protein assay was used to determine protein concentration. 20 μl of homogenate supernatant were added to sample buffer (1% SDS, 1% β-mercaptoethanol, 5% glycerol, 25 mM Tris-HCl (pH 6.8)) and heated at 40°C for 1 h to denature the proteins. After that, 10 μl of 0.005% bromophenol blue were added. A total of 3.8 μg of protein was electrophoresed on 4% stacking and 12% separating SDS-polyacrylamide gel, and transferred to the nitrocellulose membrane. Pre-stained molecular weight markers (Roth) were used to estimate position of protein bands. To examine the expressions of cofilin protein in CHO AA8 cells, we used an anti-cofilin antibody produced in rabbit (Sigma Aldrich). The membrane was blocked for 24 h at 4°C with TBS buffer (25 mM Tris-HCl (pH 8.0), 137 mM NaCl, 2.7 mM KCl) containing 5% nonfat dry milk powder. Primary antibodies were added at dilution in TBS containing 5% nonfat dry milk powder and incubated 1 h at room temperature. The membrane was washed twice with TBS. Incubation with a secondary antibody of anti-rabbit IgG (whole molecule)-alkaline phosphatase produced in goat (Sigma Aldrich) was performed for 1 h at room temperature. Protein bands were visualized using NBT/BCIP Ready-to-Use Tablets (Roche). Western blot images were quantitated using Quantity One Basic software (Ver3.6.5; Bio-Rad).

The isolation of nuclei. The cell pellet was suspended in the homogenizing solution (0.5 M Tris-HCl (pH 7.5), 0.5 M $CaCl_2$, 1M saccharose, 0.5 M $MgCl_2$, Nonidet, 2-mercaptoethanol). Homogenate was crushed in Potter's homogenizer on ice centrifuged at 700 g for 10 min., at 4°C. Afterwards, cell precipitation was suspended in 1ml of the homogenizing solution and slowly added to the cooled solution containing 0.5 M Tris-HCl (pH 7.5), 0.5M KCl, 1 M saccharose, glycerol, 0.5 M $MgCl_2$ and 2-mercaptoethanol. The mixture was centrifuged at 700 g for 10min., at 4°C.

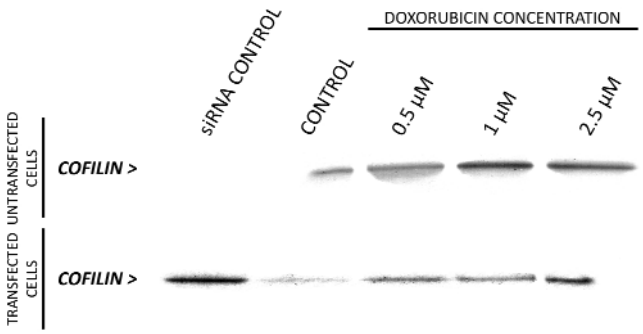

Fig. 1. Expression of cofilin in untransfected and transfected with $siRNA_{Cfl1}$ CHO AA8 cells exposed to 0.5, 1 and 2.5 μM doxorubicin. After treatment, cofilin protein were analyzed by Western blot using specific antibodies. After transfection of CHO AA8 cells with $siRNA_{Cfl1}$ the expression of cofilin was decreased to a level 48.7%, 46.9%, 59.6%, and 49.46% in control and doxorubicin treated cells, respectively.

Finally, the supernatant was carefully decanted and precipitation was suspended in 1ml of fixing solution (4% (v/v) PFA in PBS, pH 7.4).

Fluorescence microscopy. The CHO AA8 cells grown on sterile glass coverslips were fixed with 4% paraformaldehyde in PBS, pH 7.4 (20 min., room temperature) and then stained for F-actin with phalloidin/Alexa Fluor 488 (Molecular Probes) in PBS containing 20% methanol (20 min., room temperature). Labeling of cofilin using an anti-cofilin antibody produced in rabbit (Sigma Aldrich) was performed for 1 h at room temperature. This was followed by rinse in PBS-BSA, three times for 5 min. and incubation with a goat anti-rabbit IgG-TR secondary antibody (Santa Cruz Biotechnology) for 1 h at room temperature. Cell nuclei were stained with DAPI (Sigma Aldrich). Labeled cells were observed using Nikon C1 laser-scanning confocal microscopy system (Nikon). Images were captured using Nikon EZ-C1 software (Ver3.80; Nikon)

TUNEL assay. The TUNEL (terminal deoxynucleotidyl transferase-mediated dUTP-biotin nick end-labeling) method was used to detect DNA strand breaks. TUNEL was carried out according to manufacturer's instruction, with the following modifications: cell fixation was performed on ice (15 min., 1% formaldehyde) and was followed by cell permeabilization in 70% ethanol (30 min., on ice). After TUNEL-FITC staining, the propidium iodide (PI)/RNase solution was added to detect the stage of cell cycle. Analyses were performed on a Becton-Dickinson FACScan machine. For the analysis of DNA content, doublets were excluded from the final analysis using linear plots of FL2-A *vs* FL2-W. The fractions of cells in G0/G1, S, G2/M, cells with a DNA content of more than 4n and less than 2n (apoptotic DNA) were indentified. Data analysis was carried out using FlowJo cell cycle analysis software (Tree Star).

Annexin V-FITC/7-AAD assay. Annexin V-FITC apoptosis detection kit (BD Pharmingen) was used to assess phosphatidylserine externalization. Nuclei were counterstained with 7-AAD. The assay was performed according to manufacturer's instruction. Briefly, cells were trypsinized and centrifuged (300 g for 5 min.). Following supernatant removal, 195 μl of binding buffer and 5 μl of annexin V-FITC were added. The cells were incubated for 15 min. at room temperature, in dark. After centrifugation (300 g for 5 min.) and removal of supernatant, 190 μl of binding buffer and 10 μl of 7-AAD were added to the cell pellet For flow cytometric analyses the Becton-Dickinson FACScan was used.

F-actin and cofilin content in whole cells and cell nuclei. The CHO AA8 cells and isolated cell nuclei were fixed with 1% formaldehyde (15 min., on ice) and permeabilized in 70% methanol (30 min., on ice). Labeling of cofilin was performed using anti-cofilin rabbit polyclonal antibody (Sigma Aldrich) for 1 h at room temperature. After 40 min. the cells were stained with Alexa Fluor 488-conjugated phalloidin (Molecular Probes) for 20 min. at room temperature. This was followed by rinse in PBS-BSA, three times for 5 min. and incubation with PE(ab')2 donkey anti-rabbit IgG (BD) for 1 h at room temperature. Cell nuclei were stained with 7-AAD (BD). For flow cytometric analyses the Becton-Dickinson FACScan was used.

Statistical analysis. The Statistical analyses were performed by Mann-Whitney U test using GraphPad Prism software (Ver4.0; GraphPad software). Results were considered significant at a p value of <0.05.

Results

Western blotting

The effect of $siRNA_{Cfl1}$ on the expression of cofilin in CHO AA8 cells was examined by Western blotting using specific antibodies. Western blotting analysis showed significant reduction in the expression of cofilin in $siRNA_{Cfl1}$ transfected cells exposed to 0.5, 1 and 2.5 μM doxorubicin. As shown in Fig. 1, the expression of cofilin was decreased to a level 48.7%, 46.9%, 59.6%, and 49.46% for $siRNA_{Cfl1}$ transfected control cells and cofilin-1 (nonmuscle) knock-down cells treated with doxorubicin at doses 0.5, 1 and 2.5 μM, respectively.

Annexin V-FITC/7-AAD assay

To estimate if cofilin-1 down-regulation in CHO AA8 cells induces apoptosis, the flow cytometric analysis of cells stained with FITC-conjugated annexin V and 7-AAD as apoptotic/necrotic factor was used. After exposition of untransfected CHO AA8 cells to various doses of doxorubicin, the decrease in number of viable cells was observed. Additionally, there was also observed doxorubicin dose dependent increase in the number of annexin V-positive/7-AAD-negative, annexin V-FITC/7-AAD-double positive, and annexin V-FITC-negative/7-AAD-positive cells. Moreover, the most of cells were apoptotic (both early and late) and necrotic according to doxorubicin doses used (Fig. 2A).

As shown in Fig. 2D, the down-regulation of cofilin by $siRNA_{Cfl1}$ did not significantly increase both early and late apoptosis, but also necrosis in control and cells treated with various doses of doxorubicin (determined by annexin V-positive/7-AAD-negative, annexin V-FITC/7-AAD-double positive and annexin V-FITC-negative/7-AAD-positive cells, respectively).

Cell cycle analysis

Cell cycle analysis of untransfected cells revealed doxorubicin dose dependent increase of sub-G1 phase, but

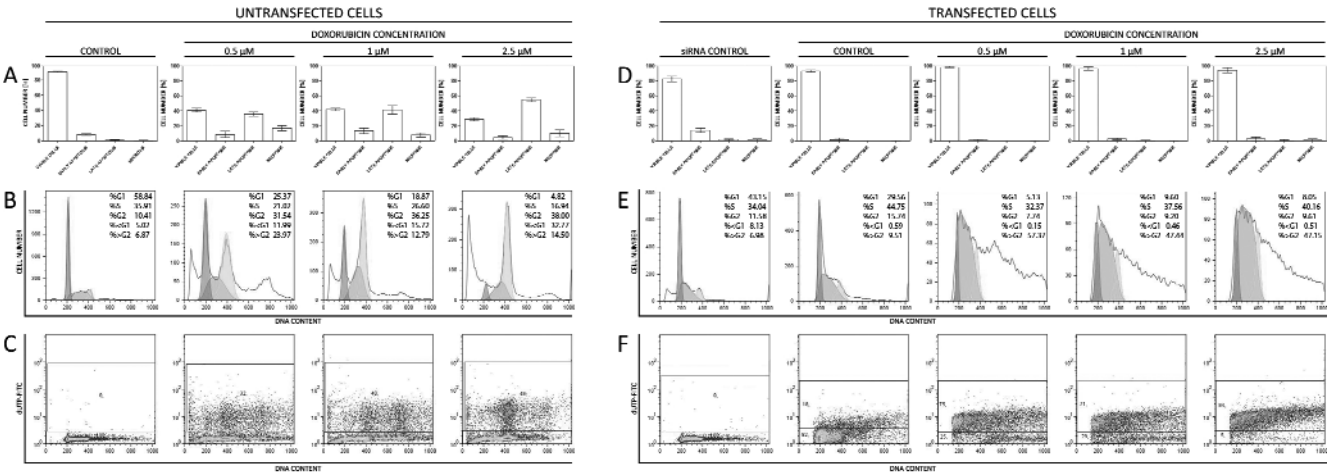

Fig. 2. (**A**) Flow cytometry analysis of cell death using double staining with 7-AAD and Annexin V-FITC after exposure of untransfected CHO AA8 cells to various doxorubicin doses. Apoptosis was evaluated after treating untransfected CHO AA8 cells with 0.5, 1 and 2.5 μM doxorubicin. Data are presented as medians and standard deviations. Mann-Whitney U test was used for statistical analysis. (**B**) Flow cytometry analysis of cell cycle in untransfected cells exposed to various doxorubicin doses. Cell cycle was analyzed after treating untransfected CHO AA8 cells with 0.5, 1 and 2.5 μM doxorubicin. Representative cell cycle histograms present DNA content in x axis and cell number in y axis. The numbers represent the percentages of cells in each phase of cell cycle. (**C**) Flow cytometry analysis of DNA fragmentation in untransfected CHO AA8 cells after exposition to various doxorubicin doses. Terminal deoxynucleotidyl transferase-mediated dUTP nick end-labeling (TUNEL) assay was performed after treating untransfected CHO AA8 cells with 0.5, 1 and 2.5 μM doxorubicin. Representative flow cytometry plots present DNA content in x axis and dUTP-FITC staining in y axis. The numbers represent the percentages of TUNEL-positive cells. (**D**) Flow cytometry analysis of cell death using double staining with 7-AAD and Annexin V-FITC after exposure of transfected with $siRNA_{Cfl1}$ CHO AA8 cells to various doxorubicin doses. Apoptosis was evaluated after treating cofilin-1 (nonmuscle) down-regulated CHO AA8 cells with 0.5, 1 and 2.5 μM doxorubicin. Data are presented as medians and standard deviations. Mann-Whitney U test was used for statistical analysis. (**E**) Flow cytometry analysis of cell cycle in transfected with $siRNA_{Cfl1}$ cells exposed to various doxorubicin doses. Cell cycle was analyzed after treating cofilin-1 (nonmuscle) down-regulated CHO AA8 cells with 0.5, 1 and 2.5 μM doxorubicin. Representative cell cycle histograms present DNA content in x axis and cell number in y axis. The numbers represent the percentages of cells in each phase of cell cycle. (**F**) Flow cytometry analysis of DNA fragmentation in $siRNA_{Cfl1}$ transfected CHO AA8 cells after exposition to various doxorubicin doses. Terminal deoxynucleotidyl transferase-mediated dUTP nick end-labeling (TUNEL) assay was performed after treating cofilin-1 (nonmuscle) down-regulated CHO AA8 cells with 0.5, 1 and 2.5 μM doxorubicin. Representative flow cytometry plots present DNA content in x axis and dUTP-FITC staining in y axis. The numbers represent the percentages of TUNEL-positive cells.

also an increase of G2/M. There was also observed the accumulation of cells in >G2 phase (Fig. 2B). Transfection with $siRNA_{Cfl1}$ resulted in the increase of the number of polyploid cells that accumulated at the expense of cells in G1, but here the analysis did not show the sub-G1 peak (Fig. 2E).

TUNEL assay

As shown in Fig. 2C, for untransfected CHO AA8 cells exposed to various doses of doxorubicin, an increase of DNA fragmentation corresponding to doxorubicin concentration was observed. We also found the same correlation for $siRNA_{Cfl1}$ transfected cells exposed to various doses of doxorubicin, but here DNA fragmentation was greater (Fig. 2F).

Fluorescence microscopy

To estimate the fluorescence of F-actin and cofilin, the confocal microscopy was used. The images of untransfected cells not treated with doxorubicin showed the network of peripheral F-actin and arrays of actin stress fibers. The cofilin labeling was seen mainly in the cytoplasm with minor fluorescence intensity the in cell nuclei of control cells, which were rather single and oval. Some of them were kidney-shaped, characteristic for CHO AA8 fibroblasts (Fig. 3A). The double staining of F-actin and cofilin showed doxorubicin dose dependent tendency to formation the multinucleated giant cells, but also the increase of fluorescence intensity of cofilin in cell nuclei. Additionally, in the nuclear region of multinucleated giant cells, the areas without F-actin and DNA staining similar to intranuclear cytoplasmic inclusions were seen. After 0.5 μM doxorubicin treatment, the untrasfected CHO AA8 cells revealed the overlapping pattern of F-actin and cofilin staining within nuclei. Moreover, multinucleated cells with expanded F-actin cytoskeleton and extended stress fibers were observed (Fig. 3B). Beside of multinucleated cells with extended network of F-actin and stress fibers as shown in Fig. 3C, the exposure of untransfected cells to doxorubicin dose of 1 and 2.5 μM showed also hallmarks of apoptosis,

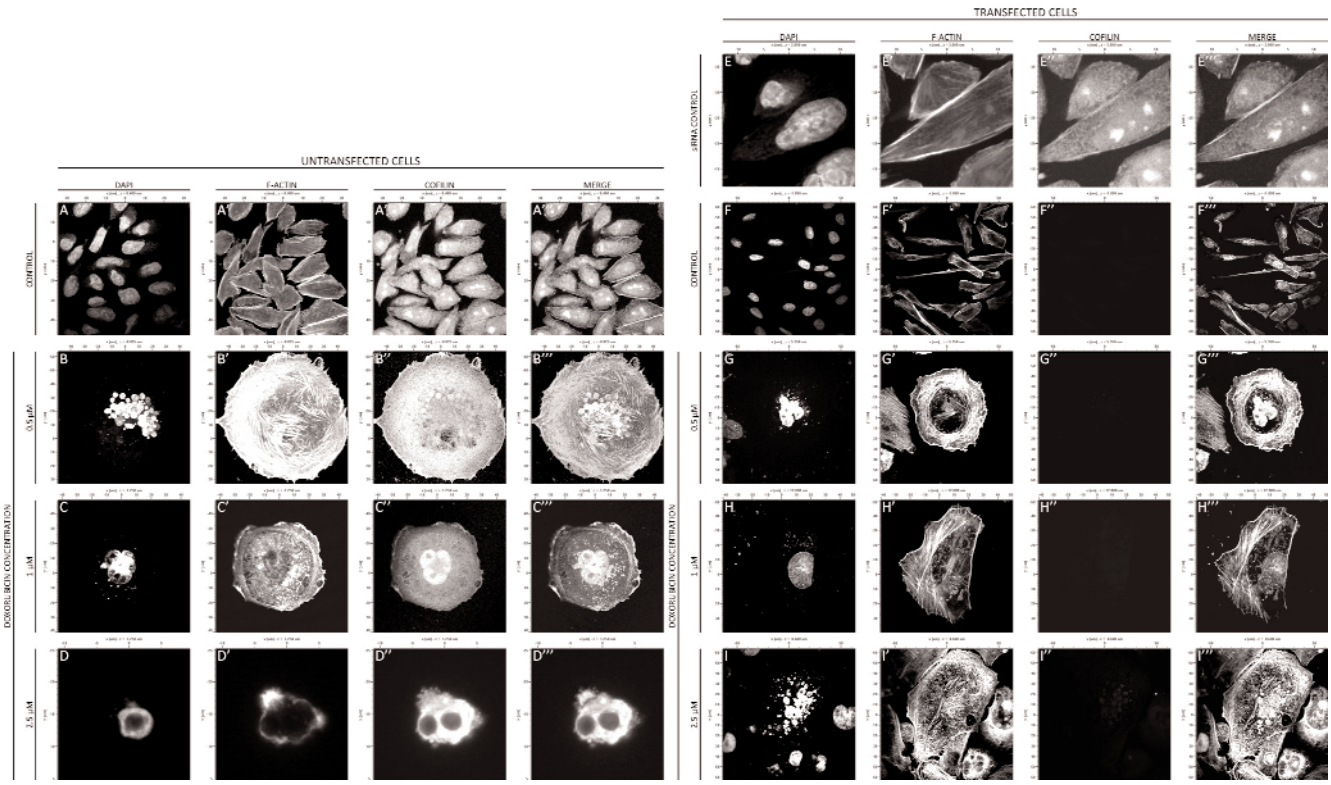

Fig. 3. (**A-D**) Doxorubicin induced morphological changes in untransfected CHO AA8 cells. The cells were treated with 0.5, 1 and 2.5 μM doxorubicin and immunolabeled for the presence of cofilin and F-actin. Cell nuclei were labeled with DAPI. (**A**) Control; (**B**) 0.5 μM doxorubicin; (**C**) 1 μM doxorubicin; (**D**) 2.5 μM doxorubicin. (**E-I**) Doxorubicin induced morphological changes in transfected with $siRNA_{Cfl1}$ CHO AA8 cells. The cells were treated with 0.5, 1 and 2.5 μM doxorubicin and immunolabeled for the presence of cofilin and F-actin. Cell nuclei were labeled with DAPI. After transfection of CHO AA8 cells with $siRNA_{Cfl1}$ the cofiln expression was not observed. (**E**) siRNA control (**F**) Control; (G) 0.5 μM doxorubicin; (**H**) 1 μM doxorubicin; (**I**) 2.5 μM doxorubicin.

including plasma membrane blebbing, chromatin marginalization and fragmentation of DNA. Among cells with features of apoptosis, we found positive staining of both F-actin and cofilin in apoptotic bodies (Fig. 3D).

After transfection of CHO AA8 cells with $siRNA_{Cfl1}$ the cofiln expression was not seen. We also did not rather observe nuclear localization of F-actin. Additionally, the data presented here demonstrated the doxorubicin dependent increase in the number of giant cells with micronucleation. In transfected CHO AA8 cells we have also noticed thinner actin filaments in comparison with those observed in untransfected cells. Control cells transfected with $siRNA_{Cfl1}$ were extended with characteristic lamellipodia. Moreover, these cells were characterized by expanded F-actin cytoskeleton but also by waved actin filaments in few cells (Fig. 3E). After 0.5 μM doxorubicin treatment of transfected cells, multinucleated giant cells exhibited more expanded network of F-actin as shown in control. We have also observed waved actin filaments and the lack of F-actin in perinuclear area (Fig. 3F). Exposure of $siRNA_{Cfl1}$ transfected cells to 1 μM doxorubicin caused further waving of F-actin and extension of perinuclear area without F-actin. We have also observed short, strong waved lengths of F-actin, mostly in perinuclear area (Fig. 3G). After exposition of transfected cells to 2.5 μM doxorubicin we observed not only fragmentation, but also depolymerization of F-actin (Fig. 3H).

Flow cytometric assay of F-actin and cofilin content in whole cells

To estimate F-actin and cofilin content in whole cells the flow cytometric analysis was used. The analysis of F-actin content in untransfected CHO AA8 cells revealed its doxorubicin dose dependent increase. In control cells we observed one homogenous population of cells with mean fluorescence intensity (MFI) of 283. After doxorubicin treatment beside cells with very low expression of F-actin (31% with MFI of 18, 25% with MFI of 15, and 21% with MFI of 16 in 0.5, 1 and 2.5 μM doxorubicin, respectively) there were observed populations with its relative high expression (29% with MFI of 340 and 40% with MFI of 1439, 75% with MFI of 795, and 79% with MFI of 981 in 0.5, 1 and 2.5 μM doxorubicin, respectively) (Fig.

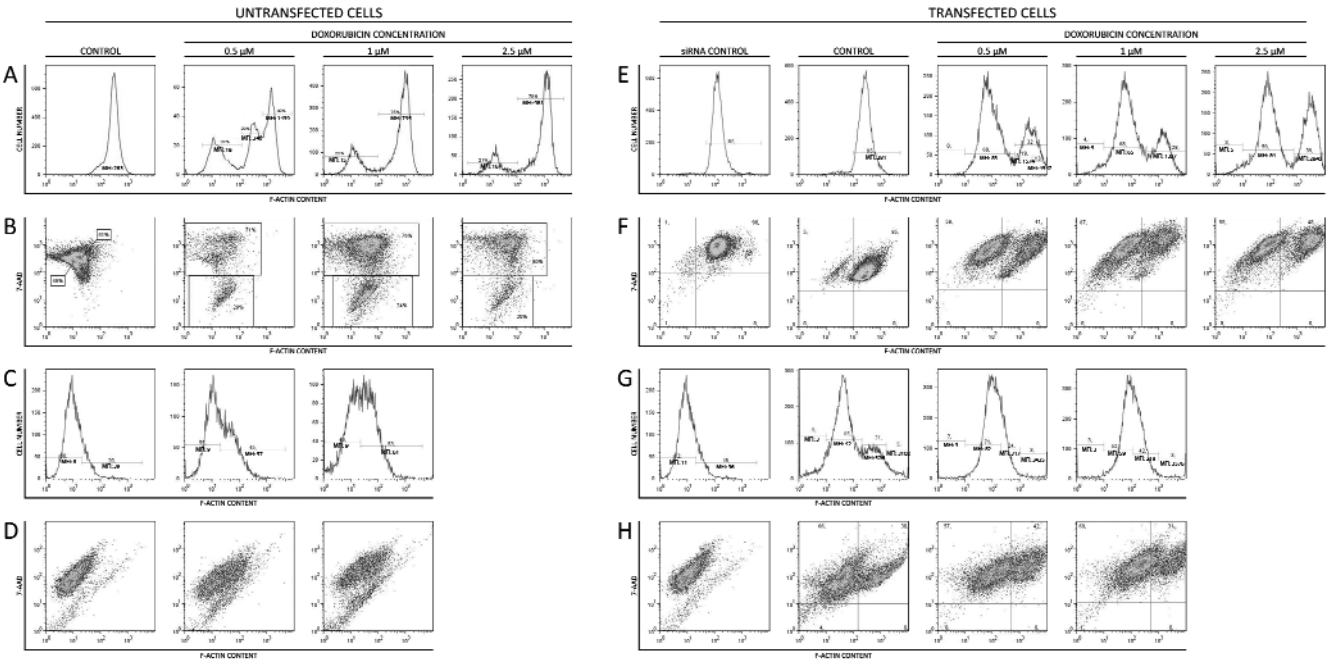

Fig. 4. (**A-D**) Flow cytometry analysis of F-actin content in whole cells and isolated nuclei of untransfected CHO AA8 cells. F-actin content was analyzed after treating untransfected CHO AA8 cells with 0.5, 1 and 2.5 μM doxorubicin. (**A**) Flow cytometry analysis of F-actin content in whole untransfected cells. Representative flow cytometry histograms present F-actin content in x axis and cell number in y axis. The numbers represent the percentages of cells; MFI - mean fluorescence intensity. (**B**) The relationship between nuclear DNA and F-actin content in whole untransfected cells. Representative flow cytometry plots present F-actin content in x axis and 7-AAD in y axis. The numbers represent the percentages of cells. (**C**) Flow cytometry analysis of F-actin content in isolated nuclei of untransfected cells. Representative flow cytometry histograms present F-actin content in x axis and cell number in y axis. The numbers represent the percentages of nuclei; MFI - mean fluorescence intensity. (**D**) The relationship between nuclear DNA and F-actin content in isolated nuclei of untransfected cells. Representative flow cytometry present F-actin content in x axis and 7-AAD in y axis. (**E-H**) Flow cytometry analysis of F-actin content in whole cells and isolated nuclei of transfected with $siRNA_{Cfl1}$ CHO AA8 cells. F-actin content was analyzed after treating transfected with $siRNA_{Cfl1}$ CHO AA8 cells with 0.5, 1 and 2.5 μM doxorubicin. (**E**) Flow cytometry analysis of F-actin content in whole transfected with $siRNA_{Cfl1}$ cells. Representative flow cytometry histograms present F-actin content in x axis and cell number in y axis. The numbers represent the percentages of cells; MFI - mean fluorescence intensity. (**F**) The relationship between nuclear DNA and F-actin content in whole transfected with $siRNA_{Cfl1}$ cells. Representative flow cytometry plots present F-actin content in x axis and 7-AAD in y axis. The numbers represent the percentages of cells. (**G**) Flow cytometry analysis of F-actin content in isolated nuclei of transfected with $siRNA_{Cfl1}$ cells. Representative flow cytometry histograms present F-actin content in x axis and cell number in y axis. The numbers represent the percentages of nuclei; MFI - mean fluorescence intensity. (**H**) The relationship between nuclear DNA and F-actin content in isolated nuclei of transfected with $siRNA_{Cfl1}$ cells. Representative flow cytometry plots present F-actin content in x axis and 7-AAD in y axis. The numbers represent the percentages of nuclei.

4A). In the case of cofilin content in untrasfected cells, the cytometric analysis showed the appearance of cell populations with its relatively high expression (68%, 30%, 65% in 0.5, 1 and 2.5 μM doxorubicin, respectively) (Fig. 5A).

The flow cytometric analysis of F-actin content in $siRNA_{Cfl1}$ transfected CHO AA8 cells showed one homogenous population of cells with mean fluorescence intensity (MFI) of 278 in control. After doxorubicin treatment the cell number with low expression of F-actin was: 68%, 68%, and 59% in 0.5, 1 and 2.5 μM doxorubicin, respectively. However, in the cells treated with doxorubicin in concentration of 0.5 μM, there was also observed a population of cells with relative high fluorescence intensity (13%, FI: 4547) (Fig. 4E). Moreover, the flow cytometric analysis of cofilin content in $siRNA_{Cfl1}$ transfected CHO AA8 cells revealed the lack of cofilin expression in control cells, but also significant down-regulation of cofilin expression in cells treated with doxorubicin doses used (Fig. 5E).

Flow cytometric assay of F-actin and cofilin content in isolated nuclei

In the case of the flow cytometric analysis in isolated nuclei, the loss of material during purification unabled us to receive reliable results at 2.5 μM doxorubicin concentration in both $siRNA_{Cfl1}$ transfected and untransfected CHO AA8 cells. In untransfected cells we found the doxorubicin dose dependent increase in both F-actin and cofilin content and their correlation with DNA content (Fig. 4C, D, Fig. 5C, D). After treat-

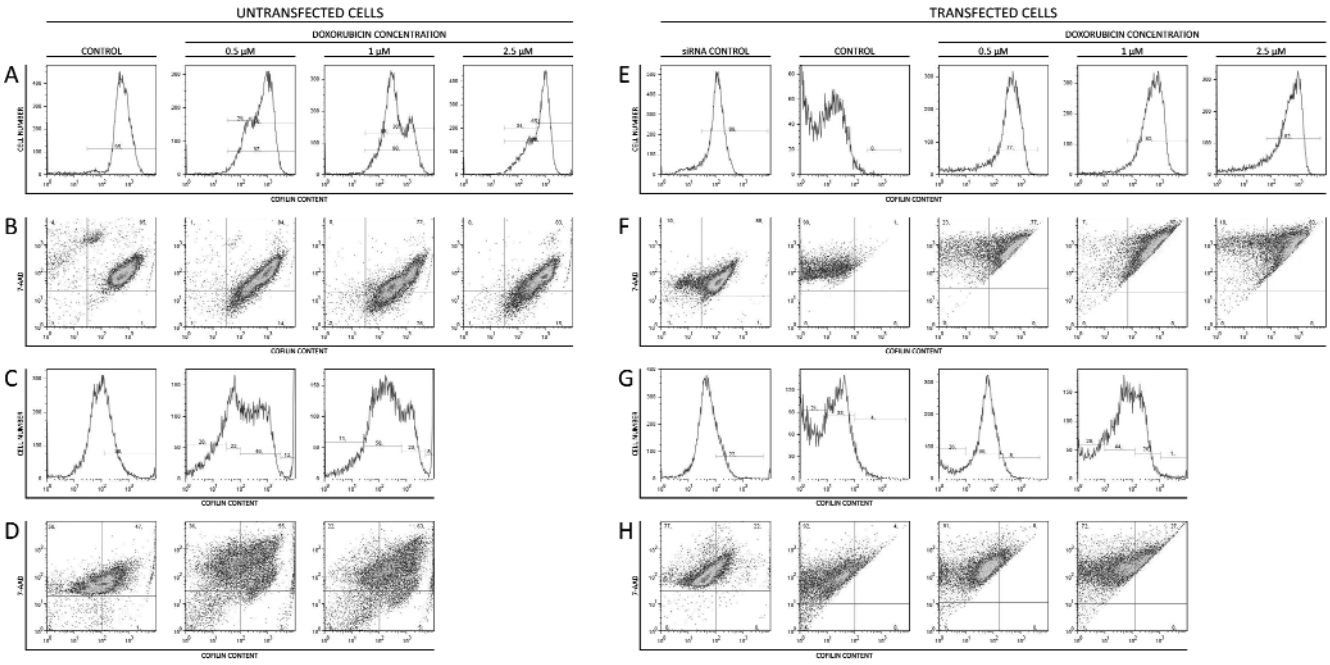

Fig. 5. (**A-D**) Flow cytometry analysis of cofilin content in whole cells and isolated nuclei of untransfected CHO AA8 cells. Cofilin content was analyzed after treating untransfected CHO AA8 cells with 0.5, 1 and 2.5 μM doxorubicin. (**A**) Flow cytometry analysis of cofilin content in whole untransfected cells. Representative flow cytometry histograms present cofilin content in x axis and cell number in y axis. The numbers represent the percentages of cells. (**B**) The relationship between nuclear DNA and cofilin content in whole untransfected cells. Representative flow cytometry plots present cofilin content in x axis and 7-AAD in y axis. The numbers represent the percentages of cells. (**C**) Flow cytometry analysis of cofilin content in isolated nuclei of untransfected cells. Representative flow cytometry histograms present cofilin content in x axis and cell number in y axis. The numbers represent the percentages of nuclei. (**D**) The relationship between nuclear DNA and cofilin content in isolated nuclei of untransfected cells. Representative flow cytometry plots present cofilin content in x axis and 7-AAD in y axis. (**E-H**) Flow cytometry analysis of cofilin content in whole cells and isolated nuclei of transfected with $siRNA_{Cfl1}$ CHO AA8 cells. Cofilin content was analyzed after treating transfected with $siRNA_{Cfl1}$ CHO AA8 cells with 0.5, 1 and 2.5 μM doxorubicin. (**E**) Flow cytometry analysis of cofilin content in whole transfected with $siRNA_{Cfl1}$ cells. Flow Representative flow cytometry histograms present cofilin content in x axis and cell number in y axis. The numbers represent the percentages of cells. (**F**) The relationship between nuclear DNA and cofilin content in whole transfected with $siRNA_{Cfl1}$ cells. Representative flow cytometry plots present cofilin content in x axis and 7-AAD in y axis. The numbers represent the percentages of cells. (**G**) Flow cytometry analysis of cofilin content in isolated nuclei of transfected with $siRNA_{Cfl1}$ cells. Representative flow cytometry histograms present cofilin content in x axis and cell number in y axis. The numbers represent the percentages of nuclei. (**H**) The relationship between nuclear DNA and cofilin content in isolated nuclei of transfected with $siRNA_{Cfl1}$ cells. Representative flow cytometry plots present cofilin content in x axis and 7-AAD in y axis. The numbers represent the percentages of nuclei.

ment with 0.5 μM doxorubicin we observed two population of cell nuclei, 46% and 12% (total 58%), with relative high expression of cofilin, whereas in doxorubicin concentration 1 μM, two populations with higher cofilin expression: 23% and 8% (total 31%) were noticed (Fig. 5C).

The flow cytometric analysis of F-actin content in isolated nuclei of $siRNA_{Cfl1}$ transfected CHO AA8 cells showed two populations of cells (21% and 5%; total 26%) in control, with mean fluorescence intensity of 734. At doxorubicin dose 0.5 μM, two populations of nuclei (24% and 3%; total 27%) with mean fluorescence intensity of 413 were observed. At doxorubicin dose 1.0 μM, two populations of cells (42% and 3%; total 26%) with mean fluorescence intensity of 266 were observed (Fig. 4G). Moreover, the flow cytometric analysis of cofilin content in isolated nuclei of $siRNA_{Cfl1}$ transfected CHO AA8 cells revealed only low percentage of nuclei with expression of cofilin in control and doxorubicin dose 0.5 μM (4% and 8% populations, respectively). At doxorubicin dose 1 μM, 26% population of cell nuclei with relative low cofilin expression was observed. However, flow cytometric analysis revealed 1% population with relative high expression of cofilin at 1 μM doxorubicin dose (Fig. 5G).

Discussion

We have previously reported that doxorubicin kills cells via both apoptosis and mitotic catastrophe [29], but also may trigger cell response including senes-

cence [39-41]. Moreover, our data showed that actin is not only involved in apoptosis but also in mitotic catastrophe in CHO AA8 cell line [29-30]. It was also suggested that the mechanism of doxorubicin action is dose dependent. As it was shown, low concentrations of doxorubicin induced senescence and/or mitotic catastrophe whereas high doses promoted apoptosis in different cell lines [40,42-44]. The mechanism of mitotic catastrophe process is still poorly understood and intensively investigated. However, some reports describe mitotic catastrophe as an abnormal mitosis in which multinucleated giant cells are formed [34-35,37-38]. In other studies this mode of cell death is also linked with polyploidy [40,45-47]. As it was shown here, after induction of cell death with doxorubicin treatment, two populations of cells were observed: with the morphology of cells undergoing apoptosis and multinucleated giant cells, characteristic for mitotic catastrophe. Moreover, results presented here indicate that besides actin, also cofilin may be involved in these two cell death pathways. The proteins of ADF/cofilin family are expressed probably in all eukaryotes, with three forms in mammalian cells: ADF, cofilin-1 (the major isoform of cofilin in non-muscle cells) and cofilin-2 (the major isoform of cofilin in muscle cells). Both ADF and cofilin-1 play a major role in the modulation of actin dynamics. ADF is more efficient in monomer sequestering, whereas cofilin in nucleation and severing [48]. In this report we used RNAi technique to demonstrate the effect of cofilin on nuclear and cytoplasmic actin pool in CHO AA8 cells. In present study, after doxorubicin treatment of untransfected with $siRNA_{Cfl1}$ CHO AA8 cells, both apoptosis and mitotic catastrophe were observed. In cells with apoptotic features we observed colocalisation of F-actin and cofilin mostly in apoptotic blebs. However, our immunofluorescence studies revealed not only the high expression of cofilin in apoptotic bodies but also its high fluorescence intensity in the area of chromatin marginalization. Moreover, our flow cytometry studies in untransfected cells showed doxorubicin dose dependent increase of apoptotic cells, mostly annexin V-FITC/7-AAD-double positive. It allows to suppose that cofilin mediates apoptosis in the response to doxorubicin. Similarly, Huot *et al*. observed actin at the border of the apoptotic blebs whereas Levee *et al*. showed accumulation of F-actin in the area of apoptotic body formation and suggested that the reorganization of F-actin network is essential for this process [49-50]. Moreover, Chua *et al*. reported that cofilin has an important function during the initiation phase of apoptosis. As it was shown, cofilin mediates apoptosis in the response to stauroporine through its translocation to mitochondria, displaying typical for this mode of cell death morphological changes such as diffuse cytochrome c staining in cytoplasm, nuclear condensation and fragmentation [51]. It was also suggested that oxidant-induced apoptosis and mitochondrial integrity can be regulated through oxidation of cofilin [52]. In contrast, our immunofluorescence data showed the lack of cofilin in the cell nuclei of $siRNA_{Cfl1}$ transfected CHO AA8 cells. Moreover, these observations were confirmed by flow cytometry analysis in isolated nuclei, which agree with thesis that actin itself has no nuclear-localization sequence, but bound to cofilin does [48]. Because actin is essential in chromatin-remodeling complexes and consequently in gene expression [14, 53], we may suggest that different mechanisms of chromatin reorganization are involved in apoptosis and mitotic catastrophe. Additionally, we previously reported that mitotic catastrophe probably ends in apoptosis [30]. The data obtained here shed new light on these two processes. The flow cytometry analysis showed apoptosis only in untrasfected cells whereas mitotic catastrophe was observed in both $siRNA_{Cfl1}$ transfected and untransfected cells. In addition, our fluorescence studies revealed the lack of F-actin in the nuclei of cofilin-1 (nonmuscle) down-regulated cells which may suggest an independence of mitotic catastrophe from F-actin content in cell nucleus. In this point of view, these two modes of cell death seems to be independent processes from each other and allow to suggest that cofilin is required for initiation of apoptosis process.

In conclusion, our results showed that doxorubicin induces both apoptosis and mitotic catastrophe in CHO AA8 cell line. However, the results presented here allow us to suggest that the cofilin has apoptosis-inducing ability. We also suggest that the changes in the nuclear expression of cofilin are related to F-actin shifting from cytoplasm to nucleus and also to its intranuclear reorganization. Moreover, we suggest that mitotic catastrophe is independent from F-actin content in the cell nucleus and different mechanisms of chromatin reorganization are involved in apoptosis and mitotic catastrophe. Furthermore, we may suppose that mitotic catastrophe and apoptosis are different processes from each other.

Acknowledgements: The study was supported by grant No. 401224534 from the Polish Ministry of Science and Higher Education.

References

[1] Amann KJ, Pollard TD. Cellular regulation of actin network assembly. *Curr Biol.* 2000;10:R728-30.
[2] Paavilainen VO, Bertling E, Falck S, Lappalainen P. Regulation of cytoskeletal dynamics by actin-monomer-binding proteins. *Trends Cell Biol.* 2004;14:386-94.
[3] Pollard TD, Blanchoin L, Mullins RD. Molecular mechanisms controlling actin filament dynamics in nonmuscle cells. *Annu Rev Biophys Biomol Struct.* 2000;29:545-76

[4] dos Remedios CG, Chhabra D, Kekic M *et al*. Actin binding proteins: regulation of cytoskeletal microfilaments. *Physiol Rev*. 2003;83:433-73.
[5] Rao J, Li N. Microfilament actin remodeling as a potential target for cancer drug development. *Curr Cancer Drug Targets*. 2004;4:345-54.
[6] Grzanka A, Grzanka D, Zuryń A, Grzanka AA, Safiejko-Mroczka B. Reorganization of actin in K-562 and HL-60 cells treated with taxol. *Neoplasma.* 2006;53:56-61.
[7] Grzanka D, Grzanka A, Izdebska M, Gackowska L, Stepien A, Marszalek A. Actin reorganization in CHO AA8 cells undergoing mitotic catastrophe and apoptosis induced by doxorubicin. *Oncol Rep.* 2010;23:655-63.
[8] Chen H, Bernstein BW, Bamburg JR. Regulating actin-filament dynamics in vivo. *Trends Biochem Sci.* 2000;25:19-23.
[9] Grzanka D, Domaniewski J, Grzanka A. Effect of doxorubicin on actin reorganization in Chinese hamster ovary cells. *Neoplasma.* 2005;52:46-51.
[10] Grzanka A, Grzanka D, Orlikowska M. Cytoskeletal reorganization during process of apoptosis induced by cytostatic drugs in K-562 and HL-60 leukemia cell lines. *Biochem Pharmacol.* 2003;66:1611-7.
[11] Grzanka A, Grzanka D, Orlikowska M. Fluorescence and ultrastructural localization of actin distribution patterns in the nucleus of HL-60 and K-562 cell lines treated with cytostatic drugs. *Oncol Rep.* 2004;11:765-70.
[12] Olave IA, Reck-Peterson SL, Crabtree GR. Nuclear actin and actin-related proteins in chromatin remodeling. *Annu Rev Biochem.* 2002;71:755-81.
[13] McDonald D, Carrero G, Andrin C, de Vries G, Hendzel MJ. Nucleoplasmic beta-actin exists in a dynamic equilibrium between low-mobility polymeric species and rapidly diffusing populations. *J Cell Biol.* 2006;172:541-52.
[14] Pederson T. As functional nuclear actin comes into view, is it globular, filamentous, or both? *J Cell Biol.* 2008;180:1061-4.
[15] Volkman LE, Talhouk SN, Oppenheimer DI, Charlton CA. Nuclear F-actin: A functional component of baculovirus-infected lepidopteran cells? *J Cell Sci.* 1992;103:15-22.
[16] Iida K, Matsumoto S, Yahara I. The KKRKK sequence is involved in heat shock-induced nuclear translocation of the 18-kDa actin-binding protein, cofilin. *Cell Struct Funct.* 1992;17:39-46.
[17] Nishida E, Iida K, Yonezawa N, Koyasu S, Yahara I, Sakai H. Cofilin is a component of intranuclear and cytoplasmic actin rods induced in cultured cells. *Proc Natl Acad Sci USA.* 1987;84:5262-6.
[18] Abe H, Nagaoka R, Obinata T. Cytoplasmic localization and nuclear transport of cofilin in cultured myotubes. *Exp Cell Res.* 1993;206:1-10.
[19] Pendleton A, Pope B, Weeds A, Koffer A. Latrunculin B or ATP depletion induces cofilin-dependent translocation of actin into nuclei of mast cells. *J Biol Chem.* 2003;278:14394-400.
[20] Vartiainen MK. Nuclear actin dynamics--from form to function. *FEBS Lett.* 2008;582:2033-40
[21] Theriot JA. Accelerating on a treadmill: ADF/cofilin promotes rapid actin filament turnover in the dynamic cytoskeleton. *J Cell Biol.* 1997;136:1165-8.
[22] Bamburg JR, Wiggan OP. ADF/cofilin and actin dynamics in disease. *Trends Cell Biol.* 2002;12:598-605.
[23] Zhou BB, Elledge SJ. The DNA damage response: putting checkpoints in perspective. *Nature.* 2000;408:433-9.
[24] Roninson IB, Broude EV, Chang BD. If not apoptosis, then what? Treatment-induced senescence and mitotic catastrophe in tumor cells. *Drug Resist Updat.* 2001;4:303-13.
[25] Bree RT, Neary C, Samali A, Lowndes NF. The switch from survival responses to apoptosis after chromosomal breaks. *DNA Repair (Amst)*. 2004;3:989-95.
[26] Erenpreisa J, Cragg MS. Mitotic death: a mechanism of survival? A review. *Cancer Cell Int.* 2001;1:1.
[27] Kroemer G, Galluzzi L, Vandenabeele P *et al*. Classification of cell death: recommendations of the Nomenclature Committee on Cell Death 2009. *Cell Death Differ.* 2009;16:3-11.
[28] Stepien A, Grzanka A, Grzanka D, Andrzej Szczepanski M, Helmin-Basa A, Gackowska L. Taxol-induced polyploidy and cell death in CHO AA8 cells. *Acta Histochem.* 2010;112:62-71.
[29] Grzanka D, Grzanka A, Izdebska M, Gackowska L, Stepien A, Marszalek A. Actin reorganization in CHO AA8 cells undergoing mitotic catastrophe and apoptosis induced by doxorubicin. *Oncol Rep.* 2010;23:655-63.
[30] Grzanka D, Stepien A, Grzanka A, Gackowska L, Helmin-Basa A, Szczepanski MA. Hyperthermia-induced reorganization of microtubules and microfilaments and cell killing in CHO AA8 cell line. *Neoplasma.* 2008;55:409-15.
[31] Portugal J, Mansilla S, Bataller M. Mechanisms of drug-induced mitotic catastrophe in cancer cells. *Curr Pharm Des.* 2010;16:69-78.
[32] Castedo M, Perfettini JL, Roumier T, Andreau K, Medema R, Kroemer G. Cell death by mitotic catastrophe: a molecular definition. *Oncogene.* 2004;23:2825-37.
[33] Nitta M, Kobayashi O, Honda S, Hirota T, Kuninaka S, Marumoto T *et al*. Spindle checkpoint function is required for mitotic catastrophe induced by DNA-damaging agents. *Oncogene.* 2004;23:6548-58.
[34] King KL, Cidlowski JA. Cell cycle and apoptosis: common pathways to life and death. *J Cell Biochem.* 1995;58:175-80.
[35] Miranda EI, Santana C, Rojas E, Hernández S, Ostrosky-Wegman P, García-Carrancá A. Induced mitotic death of HeLa cells by abnormal expression of c-H-ras. *Mutat Res.* 1996;349:173-82.
[36] Heddle JA, Carrano AV. The DNA content of micronuclei induced in mouse bone marrow by gamma-irradiation: evidence that micronuclei arise from acentric chromosomal fragments. *Mutat Res.* 1977;44:63-9.
[37] Abend M, Gilbertz KP, Rhein A, van Beuningen D. Early and late G2 arrest of cells undergoing radiation-induced apoptosis or micronucleation. *Cell Prolif.* 1996;29:101-13.
[38] Dini L, Coppola S, Ruzittu MT, Ghibelli L. Multiple pathways for apoptotic nuclear fragmentation. *Exp Cell Res.* 1996;223:340-7.
[39] Rebbaa A, Zheng X, Chou PM, Mirkin BL. Caspase inhibition switches doxorubicin-induced apoptosis to senescence. *Oncogene.* 2003;22:2805-11.
[40] Eom YW, Kim MA, Park SS *et al*. Two distinct modes of cell death induced by doxorubicin: apoptosis and cell death through mitotic catastrophe accompanied by senescence-like phenotype. *Oncogene.* 2005;24:4765-77.
[41] Joyner DE, Bastar JD, Randall RL. Doxorubicin induces cell senescence preferentially over apoptosis in the FU-SY-1 synovial sarcoma cell line. *J Orthop Res.* 2006;24:1163-9.
[42] Park SS, Eom YW, Choi KS. Cdc2 and Cdk2 play critical roles in low dose doxorubicin-induced cell death through mitotic catastrophe but not in high dose doxorubicin-induced apoptosis. *Biochem Biophys Res Commun.* 2005;334:1014-21.
[43] Park SS, Kim MA, Eom YW, Choi KS. Bcl-xL blocks high dose doxorubicin-induced apoptosis but not low dose doxorubicin-induced cell death through mitotic catastrophe. *Biochem Biophys Res Commun.* 2007;363:1044-9.
[44] Mansilla S, Priebe W, Portugal J. Mitotic catastrophe results in cell death by caspase-dependent and caspase-independent mechanisms. *Cell Cycle.* 2006;5:53-60.
[45] Nagl W. Polyploidy in differentiation and evolution. *Int J Cell Cloning.* 1990;8:216-23.
[46] Nakahata K, Miyakoda M, Suzuki K, Kodama S, Watanabe M. Heat shock induces centrosomal dysfunction, and causes

non-apoptotic mitotic catastrophe in human tumour cells. *Int J Hyperthermia.* 2002;18:332-43.
[47] Erenpreisa J, Kalejs M, Ianzini F *et al*. Segregation of genomes in polyploid tumour cells following mitotic catastrophe. *Cell Biol Int.* 2005;29:1005-11.
[48] Bernstein BW, Bamburg JR. ADF/Cofilin: a functional node in cell biology. *Trends Cell Biol.* 2010;(in press).
[49] Huot J, Houle F, Rousseau S, Deschesnes RG, Shah GM, Landry J. SAPK2/p38-dependent F-actin reorganization regulates early membrane blebbing during stress-induced apoptosis. *J Cell Biol.* 1998;143:1361-73.
[50] Levee MG, Dabrowska MI, Lelli JL Jr, Hinshaw DB. Actin polymerization and depolymerization during apoptosis in HL-60 cells. *Am J Physiol.* 1996;271:C1981-92.
[51] Chua BT, Volbracht C, Tan KO, Li R, Yu VC, Li P. Mitochondrial translocation of cofilin is an early step in apoptosis induction. *Nat Cell Biol.* 2003;5:1083-9.
[52] Klamt F, Zdanov S, Levine RL *et al*. Oxidant-induced apoptosis is mediated by oxidation of the actin-regulatory protein cofilin. *Nat Cell Biol.* 2009;11:1241-6.
[53] Zheng B, Han M, Bernier M, Wen JK. Nuclear actin and actin-binding proteins in the regulation of transcription and gene expression. *FEBS J.* 2009;276:2669-85.

Submitted: 1 April, 2010
Accepted after reviews: 28 May, 2010